

IMPERFECTION SENSITIVITY AT DELAMINATION BUCKLING AND GROWTH

BERTIL STORÅKERS and KARL-FREDRIK NILSSON

Department of Solid Mechanics, Royal Institute of Technology, S-100 44 Stockholm,
Sweden

(Received 6 July 1992; in revised form 8 October 1992)

Abstract—The influence of initial geometric imperfections is analysed at buckling and crack growth in compressed composite plates with delaminations present. First, initial buckling based on bifurcation theory and postbuckling is considered for initially flat laminates with appropriate crack parameters determined. For initially deflected plates, Marguerre shallow shell theory is drawn upon and by a scaling procedure pertinent results in the case of imperfections may be generated directly from those of perfect plates. The method is based on the assumption of affinity between initial and postbuckling transverse deflections. In particular for inextensible buckling states, the method is exact while in more general cases estimates are obtained. Illustrations of the method and procedures are given for several representative cases and especially the associated accuracy of the method is delineated.

1. INTRODUCTION

Since the pioneering study by Koiter (1945), the sensitivity of geometric imperfections at buckling of structural members such as plates and shells has in essence become well understood. Thus, in particular for curved panels and shells, it is notorious that determination of critical loads based on bifurcation theory might severely underestimate collapse loads in realistic circumstances. For plates, however, the issue is not highly critical as generally at a bifurcation point, although the tangential stiffness is ordinarily reduced, it is still positive. Koiter's theory, originally based on isotropic homogeneous linear elasticity has also been generalized to apply to anisotropic material behaviour such as for composite laminates [cf. e.g. Librescu and Chang (1992)].

At the advent of laminates, however, the presence of interlaminar cracks may further reduce the stiffness and strength of compressed panels. In particular for polymer based composite structures, the initiation and growth of interfacial cracks is often due to low velocity impact. That resulting failure may be catastrophic has been explicitly demonstrated by Chai *et al.* (1983) and recently in a survey of related matters by Abrate (1991). The combination of buckling and crack growth is, however, dominant also in other situations such as for instance at thermal loading of surface layers (Evans and Hutchinson, 1984).

In an early study Chai *et al.* (1981) analysed the behaviour of an interlayer crack close to the surface in a thick compressed substrate. In this so-called thin film analysis post-buckling of cracked laminates was determined and eventual crack growth predicted based on a Griffith criterion. In this spirit many followers have discussed buckling-induced delamination growth [for recent accounts see Garg (1988), Storåkers (1989), and Hutchinson and Suo (1992)]. The approach is usually based on linear fracture mechanics with the energy release rates and its contingent mode dependence adopted as critical crack parameters. Thus subsequent to the initiation of buckling relevant parameters will eventually reach a critical state when a crack is expected to grow.

For the philosophy outlined, it is evident that the procedure will in general be non-conservative unless unavoidable geometric imperfections are taken into account. Thus the event of crack growth under steady compression might very well precede the bifurcation load at buckling. The matter has been subject to attention for the case of embedded through-width delaminations and based on column theory by e.g. Whitcomb (1986) and more recently, also including experimental aspects by Gillespie and Carlsson (1991). It is the present purpose then to analyse the matter in more general cases and in particular deduce an analytical estimation procedure. The method which is based on affinity at postbuckling,

as originally proposed for isotropic plates by Nylander (1951), might in some circumstances generate exact results.

2. FIELD EQUATIONS FOR IMPERFECT VON KARMAN PLATES

With the stated objective to analyse delamination buckling and growth in geometrically imperfect laminates, the mechanical behaviour of a von Karman plate is first considered. The two-dimensional strain tensor is composed of a combination of Föppl stretching

$$e_{\alpha\beta}^m = \frac{1}{2}(u_{\alpha,\beta} + u_{\beta,\alpha} + u_{3,\alpha}u_{3,\beta} + u_{3,\alpha}u_{3,\beta}^0 + u_{3,\beta}u_{3,\alpha}^0) \tag{1}$$

and a Kirchhoff bending term

$$e_{\alpha\beta}^b = x_3\kappa_{\alpha\beta}, \quad \kappa_{\alpha\beta} = -u_{3,\alpha\beta} \tag{2}$$

such that

$$e_{\alpha\beta} = e_{\alpha\beta}^m + e_{\alpha\beta}^b. \tag{3}$$

In (1), u_3^0 denotes the initial and u_3 the associate additional deflection in the deformed configuration as depicted in Fig. 1. The remaining variables are standard ones and Greek indices refer to in-plane quantities.

With the strain measures, $e_{\alpha\beta}^m$, $\kappa_{\alpha\beta}$, defined and conjugate resulting forces, $N_{\alpha\beta}$, and bending moments, $M_{\alpha\beta}$, introduced the principle of virtual work generates the local equilibrium equations

$$N_{\alpha\beta,\alpha} + p_\beta = 0, \tag{4}$$

$$M_{\alpha\beta,\alpha\beta} + N_{\alpha\beta}(u_{3,\alpha\beta} + u_{3,\alpha\beta}^0) + p_3 = 0. \tag{5}$$

In (4) p_α denotes in-plane tractions and p_3 transverse pressure. The associated dynamic boundary conditions reduce to

$$\left. \begin{aligned} n_\alpha N_{\alpha\beta} &= N_\beta^* \\ n_\alpha Q_\alpha + M_{nt,t} &= Q_n^* + M_{nt,t}^* \\ M_{nn} &= M_{nn}^* \end{aligned} \right\}, \tag{6}$$

Q_α being the resulting shear force related to bending moments and membrane forces by

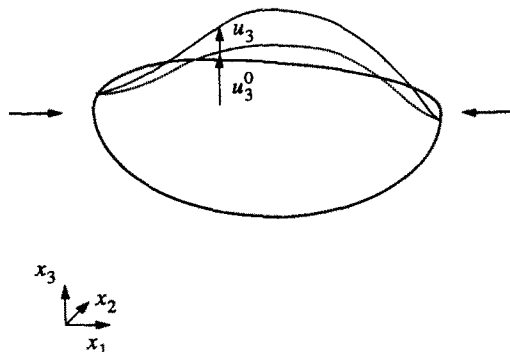


Fig. 1. Undeformed and deformed imperfect plate.

$$Q_\beta = M_{\alpha\beta,\alpha} + N_{\alpha\beta}(u_{3,\alpha} + u_{3,\alpha}^0). \quad (7)$$

In general, the constitutive properties may be defined by a strain energy function $W(e_{\alpha\beta}^m, \kappa_{\alpha\beta})$, which is not necessarily quadratic. For linear materials in particular, the constitutive equation may be expressed explicitly as:

$$\left. \begin{aligned} N_{\alpha\beta} &= A_{\alpha\beta\gamma\delta} e_{\gamma\delta}^m + B_{\alpha\beta\gamma\delta} \kappa_{\gamma\delta} \\ M_{\alpha\beta} &= B_{\alpha\beta\gamma\delta} e_{\gamma\delta}^m + D_{\alpha\beta\gamma\delta} \kappa_{\gamma\delta} \end{aligned} \right\}, \quad (8)$$

with ordinary symmetries prevailing in the stiffness tensors.

The governing equations as they stand are known in the isotropic case as the Marguerre equations (Marguerre, 1938), as here represented by an initial imperfection, u_3^0 . It is convenient to summarize by first introducing a stress-function, Φ , such that

$$N_{\alpha\beta} = \epsilon_{\alpha\gamma} \epsilon_{\beta\delta} \Phi_{,\gamma\delta}, \quad (9)$$

omitting the prescribed surface tractions for simplicity and letting $\epsilon_{\alpha\beta}$ denote the two-dimensional permutation tensor.

Then by using compatibility in (1)–(3) and satisfying (4) and (5) the resulting equations may then be written in a compact form as:

$$\left. \begin{aligned} F(\Phi, u_3) &= \epsilon_{\alpha\gamma} \epsilon_{\beta\delta} (u_{3,\alpha\beta} u_{3,\gamma\delta} + u_{3,\alpha\beta} u_{3,\gamma\delta}^0 + u_{3,\alpha\beta}^0 u_{3,\gamma\delta}) \\ G(\Phi, u_3) &= \epsilon_{\alpha\gamma} \epsilon_{\beta\delta} \Phi_{,\gamma\delta} (u_3 + u_3^0)_{,\alpha\beta} \end{aligned} \right\}, \quad (10)$$

where, as is well known (Lekhnitskii, 1981), the operators F and G are linear. If presently the constitutive properties are uncoupled, i.e. $\mathbf{B} = \mathbf{O}$ in (8), F and G decouple and at isotropy they are biharmonic.

3. AFFINITY AND IMPERFECTION SCALING

For initially deflected thin plates of Hookean material behaviour it was observed by Nylander (1951) and later accounted for by Chia (1980) that if an imperfection, $u_3^0(x_\alpha)$, is affine to the additional deflection $u_3(x_\alpha)$, i.e.

$$u_3^0 = k \cdot u_3, \quad (11)$$

k being a positive constant, then by a proper scaling the von Karman equations for a perfect plate may be recovered from the Marguerre equations.

Retaining eqn (11) and pursuing the notion in the case of anisotropy, first a transformation of relevant variables is introduced such that

$$\left. \begin{aligned} \tilde{u}_\alpha &= c_1 u_\alpha, & \tilde{u}_3 &= c_2 u_3, & \tilde{e}_{\alpha\beta}^m &= c_3 e_{\alpha\beta}^m, & \tilde{\kappa}_{\alpha\beta} &= c_4 \kappa_{\alpha\beta} \\ \tilde{N}_{\alpha\beta} &= c_5 N_{\alpha\beta}, & \tilde{M}_{\alpha\beta} &= c_6 M_{\alpha\beta}, & \tilde{\mathbf{A}} &= c_7 \mathbf{A}, & \tilde{\mathbf{B}} &= c_8 \mathbf{B}, & \tilde{\mathbf{D}} &= c_9 \mathbf{D} \\ \tilde{p}_\alpha &= c_{10} p_\alpha, & \tilde{p}_3 &= c_{11} p_3 \end{aligned} \right\}, \quad (12)$$

where the free parameters c_1 – c_{11} are to be determined. Further, the coordinates x_α may be scaled accordingly but subsequently they prove to be of no advantage in the present circumstances.

Then on introducing (11) and (12) into the governing equations (1)–(5) and (8) with the intention of formally dissolving u_3^0 , it may first be observed that the resulting system of equations to determine the c_r -parameters in (12) is redundant. On closer inspection, however,

it turns out that any solution is singular unless $c_8 = 0$, i.e. the constitutive variables in (8) must necessarily be uncoupled, $\mathbf{B} = \mathbf{O}$. In cases when $\mathbf{B} \neq \mathbf{O}$, the singularity may, however, be removed by an appropriate choice of the plate middle surface such that $\mathbf{B} = \mathbf{O}$. Staying true to von Karman kinematics the remaining variables may then be redefined accordingly but the matter is not detailed further here.

Setting $c_8 = 0$ two redundant parameters in (12) may still be chosen at will and for convenience putting $c_7 = c_9 = 1$, the remaining parameters follow as

$$c_1 = c_3 = c_5 = c_{10} = 1 + k, \quad c_2 = c_4 = c_6 = c_{11} = \sqrt{(1+k)(1+2k)}, \quad (13)$$

when u_3^0 is demanded to vanish in the transformed set of governing equations, in particular (1) and (5). The boundary conditions (6) and (7) may be scaled likewise which also applies to the conjugate kinematic boundary condition.

Then the solution for a perfect plate, \tilde{u}_i , when $u_3^0 = 0$, generates the solution, u_i , for a corresponding imperfect plate, when $u_3^0 \neq 0$, for the derived scaling procedure under the affinity assumption (11). In what circumstances the method is exact or merely approximate will be analysed below.

Denoting, for explicitness, the magnitude of a prescribed dimensionless initial imperfection by

$$\alpha = u_3^0(0)/t, \quad (14)$$

where t is the plate thickness, then by (11)–(13) the corresponding value for k is determined by

$$\alpha = \frac{k\tilde{u}_3(0)/t}{\sqrt{(1+k)(1+2k)}}, \quad (15)$$

where $\tilde{u}_3(0)$ is the deflection at the origin for the corresponding perfect plate.

4. ENERGY RELEASE RATE AND STRESS INTENSITIES AT INTERFACE CRACKS AND IMPERFECTIONS

Once the solution to an imperfect plate problem has been accomplished by means of the scaling procedure, attention is focused on the magnitude of crack parameters. For a cracked member as depicted in Fig. 2, Storåkers and Andersson (1988) have proposed a general method based on von Karman plate theory to determine the energy release rate at local crack growth. To this end the change in potential energy of the cracked member, δU , may be expressed as

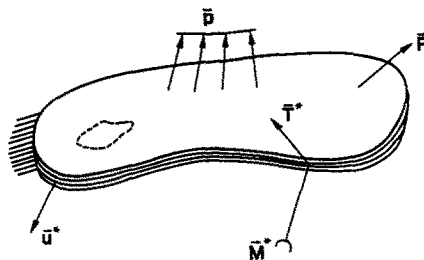


Fig. 2. Loaded plate with an interface crack.

$$\delta U = -\oint P_{\alpha\beta} \| n_\alpha n_\beta \delta a \, ds, \tag{16}$$

where

$$P_{\alpha\beta} = W\delta_{\alpha\beta} - N_{\alpha\gamma}u_{\gamma,\beta} + M_{\alpha\gamma}u_{3,\gamma\beta} \tag{17}$$

within the notation introduced above. In particular, $P_{\alpha\beta}$ may be interpreted as a plate version of Eshelby's three-dimensional energy momentum tensor satisfying the balance equations

$$P_{\alpha\beta,\alpha} - p_i u_{i,\beta} = 0. \tag{18}$$

In (16) $\| \|$ denotes the local jump at the crack front as depicted in Fig. 3 where nonuniform growth, δa , of the plane crack is assumed to be smooth along the front as measured by a curvilinear coordinate s .

In order to determine explicitly the energy released per unit area of local growth, it is favourable to align a coordinate, x_1 , locally normal to the crack front. By applying (16) and (17) the energy release rate reduces to

$$G = \| W - N_{1\alpha}u_{\alpha,1} + M_{1\alpha}u_{3,\alpha 1} \|. \tag{19}$$

To proceed, it is technically advantageous to make a local superposition of the displacement state. Thus, as recently proposed by Nilsson and Storåkers (1992), a displacement superposition at the crack front

$$\bar{u}_i^{(0)} = -u_i^{(0)} \tag{20}$$

is introduced such that the deformation vanishes locally in the uncracked part of the plate while leaving the energy release rate unaffected. This parameter then reduces to

$$G = -\sum_{k=1}^2 [(W^{(k)} + \bar{W}^{(k)} - (N_{1\alpha}^{(k)} + \bar{N}_{1\alpha}^{(k)})(u_{\alpha,1}^{(k)} + \bar{u}_{\alpha,1}^{(k)}) + (M_{1\alpha}^{(k)} + \bar{M}_{1\alpha}^{(k)})(u_{3,\alpha 1}^{(k)} + \bar{u}_{3,\alpha 1}^{(k)})], \tag{21}$$

where the barred variables originate from the superposed parts of the two cracked members.

Further, in the case of linear material behaviour and taking kinematic continuity into account, it was shown in detail within the von Karman approximation by Nilsson and Storåkers (1991) that the expression for energy release rate may be condensed to read

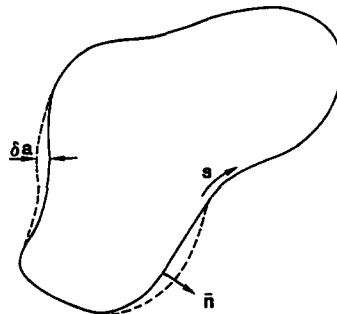


Fig. 3. Smooth growth of a plane crack.

$$G = \frac{1}{2} \sum_{k=1}^2 [(N_{1\alpha}^{(k)} + \tilde{N}_{1\alpha}^{(k)})(\varepsilon_{1\alpha}^{(k)} + \tilde{\varepsilon}_{1\alpha}^{(k)}) + (M_{11}^{(k)} + \tilde{M}_{11}^{(k)})(\kappa_{11}^{(k)} + \tilde{\kappa}_{11}^{(k)})] \quad (22)$$

in conjugate variables, where, for simplicity, $\varepsilon_{\alpha\beta} = e_{\alpha\beta}^m$.

Contemplating these prerequisites for perfect plates with one single crack present, as in Fig. 2, analysis of multiple cracks involves no fundamental difficulties as explained by Larsson (1991). Accounting for several simultaneous imperfections might, however, lead to technically rather entangled matters save when symmetries prevail. Thus in order not to obscure the present scaling principle, the analysis will be confined to the common case of a single crack and one plate member of sufficient thickness for bending to be neglected. With these features in mind, for instance for a delaminated member on a thick substrate, it is imperative to determine the corresponding energy release rate in the case of imperfections, by the scaling procedure as outlined above. Thus, for a scaled solution to a perfect plate, as represented by \tilde{u}_i , and a relative imperfection magnitude $u_3^0(0)/t$, by employing (11)–(15) it follows directly that the energy release rate is modified to

$$G = \frac{1}{2} \sum_{k=1}^2 [(\tilde{N}_{1\alpha}^{(k)} + \tilde{\tilde{N}}_{1\alpha}^{(k)})(\tilde{\varepsilon}_{1\alpha}^{(k)} + \tilde{\tilde{\varepsilon}}_{1\alpha}^{(k)})/(1+k)^2 + (\tilde{M}_{1\alpha}^{(k)} + \tilde{\tilde{M}}_{1\alpha}^{(k)})(\tilde{\kappa}_{1\alpha}^{(k)} + \tilde{\tilde{\kappa}}_{1\alpha}^{(k)})/((1+k)(1+2k))]. \quad (23)$$

Thus determination of energy release rates involves no fundamental difficulties, although as a first observation it must be concluded that evidently only partial affinity prevails.

From the viewpoint of predicting crack growth, however, it is also of interest to further decompose the energy release rate into stress intensities. For interface cracks at generally anisotropic bimetals, relevant intensities will not be real-valued and unambiguous in ordinary notation but severe coupling problems might ensue as elucidated by Suo (1990a). In a simpler situation, when anti-plane shearing modes uncouple from in-plane modes, the common stress intensity factor K_{III} may be directly read off from (23) as

$$K_{III}^2 = \sum_{k=1}^2 [\mu^{(k)} ((\tilde{N}_{12}^{(k)} + \tilde{\tilde{N}}_{12}^{(k)})(\tilde{\varepsilon}_{12}^{(k)} + \tilde{\tilde{\varepsilon}}_{12}^{(k)})/(1+k)^2)], \quad (24)$$

where $\mu^{(k)}$ are the associated shear moduli.

It is not, however, the present intention to discuss in detail the consequences of any possible material combinations but rather to investigate the potential of the present imperfection approach in simple, though practically relevant situations. Suffice it only to remember then that for isotropic bimetals, singular in-plane stresses may be expressed with the aid of complex stress intensities in the notation of Rice (1988) as

$$\sigma_{22} + i\sigma_{12} = \frac{Kr^{i\varepsilon}}{\sqrt{2\pi r}}, \quad (25)$$

where

$$K = K_1 + iK_2, \quad \varepsilon = \ln \left[\frac{(1-\beta)}{(1+\beta)} \right] / 2\pi \quad (26)$$

with β given by the Dundurs parameter

$$2\beta = \frac{\mu_1(1-2\nu_2) - \mu_2(1-2\nu_1)}{\mu_1(1-\nu_2) - \mu_2(1-\nu_1)}$$

for two Hookean materials.

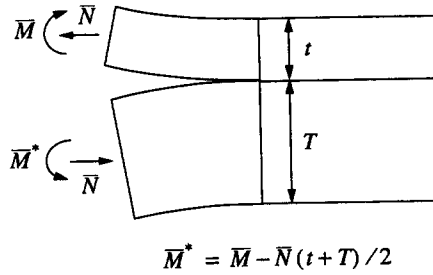


Fig. 4. Split bimaterial beam under superposed loading.

In the present setting, based on nonlinear plate theory, the explicit determination of energy release rates has by superposition been reduced to a linear beam problem. Thus, stress intensity factors are linear in ordinary beam variables and explicit determination has been carried out generally for isotropic materials by numerical means by Suo and Hutchinson (1990), when solving integral equations, and by Schapery and Davidson (1990) by a finite element technique in particular situations.

In order to characterize mode mixity, Suo and Hutchinson (1990) have defined a phase angle, Ψ , chosen as

$$|K| e^{i\Psi} = Kt^{ie} \tag{27}$$

for a split beam with thickness $t < T$ as shown in Fig. 4, local loading being appropriately superposed as delineated above. Then the phase angle Ψ will only be a function of the ratios $\bar{N}t/\bar{M}$, t/T and β . In this spirit extensive results have been given by Suo and Hutchinson (1990) for various parameter combinations and also by Suo (1990b) for orthotropic beams.

As was forecast, the present analysis will be confined to situations where one of the layers consists of a thick substrate, i.e. $t \ll T$, and furthermore to homogeneous and isotropic material behaviour. Then from a plate solution, K_{III} may be determined directly by (24) while, as has just been shown, the remaining stress intensity factors may be found from that of a superposed beam. Following the notation of Suo and Hutchinson (1990), save for a difference in sign convention for the resulting force, and in analogy with Fig. 4, the result may be expressed, with an imperfection represented by k , as

$$\begin{pmatrix} K_I \\ K_{II} \end{pmatrix} = -\frac{\bar{N}t^{-1/2}}{\sqrt{2(1+k)}} \begin{pmatrix} \cos \omega \\ \sin \omega \end{pmatrix} + \frac{\sqrt{6\bar{M}t^{-3/2}}}{\sqrt{(1+k)(1+2k)}} \begin{pmatrix} \sin \omega \\ -\cos \omega \end{pmatrix}, \tag{28}$$

where $\omega = 52.1^\circ$. This particular value of ω was found earlier by Cotterell *et al.* (1985), from a collocation method, and by Thouless *et al.* (1987) by solving an integral equation with high accuracy.

It should be emphasized though that the method of determining stress intensities in the spirit of Suo and Hutchinson (1990) and Suo (1990b) rests on asymptotic solutions based on piecewise homogeneous beam resultants. In general applications sufficiently smooth variations of load resultants and geometry parameters must prevail in order for sufficient accuracy to be retained.

5. ILLUSTRATIONS

5.1. A wide plate on a substrate under axial compression

The first model problem is shown in Fig. 5 and consists of a thin plate of thickness t , clamped to a thick substrate, $t \ll T$, with a delamination of length L . Remotely, the uncracked part of the plate is subjected to homogeneous longitudinal strain, $-\varepsilon_0$, with bending of the substrate neglected. Thus to determine relevant parameters at initial buckling and postbuckling to first order reduces to a conventional Euler buckling problem. A full

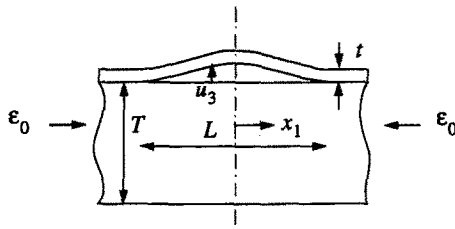


Fig. 5. Compressed wide thin plate on a substrate.

analysis, including consideration of crack growth based on a Griffith criterion, has been carried out by Chai *et al.* (1981).

Thus in the case of a Hookean perfect plate the critical strain at bifurcation becomes

$$\epsilon_{cr} = \frac{\pi^2(t/L)^2}{3(1-\nu^2)}. \tag{29}$$

At postbuckling within von Karman theory the deflection is

$$u_3(x) = u_3(0)(1 + \cos 2\pi x/L), \tag{30}$$

where, in the centre

$$u_3(0) = (2L/\pi)\sqrt{(\epsilon_0 - \epsilon_{cr})(1-\nu^2)} \tag{31}$$

as a function of the imposed loading represented by ϵ_0 .

At the crack tips, i.e. $x = \pm L/2$, the membrane strain will, as for a first order, be constant, ϵ_{cr} , at postbuckling while the corresponding curvature is

$$\kappa = \frac{4}{t}\sqrt{3(\epsilon_0 - \epsilon_{cr})\epsilon_{cr}}, \tag{32}$$

from (29)–(31).

The energy release rate is then readily shown to be

$$G = (\epsilon_0 - \epsilon_{cr})(\epsilon_0 + 3\epsilon_{cr})Et(1-\nu^2)/2. \tag{33}$$

When explicitly determining crack parameters it proves convenient to introduce dimensionless variables according to

$$G^* = \frac{2G}{\epsilon_{cr}^2 Et(1-\nu^2)}, \tag{34}$$

$$K_I^*, K_{II}^* = K_I, K_{II} \left(\frac{1-\nu^2}{\epsilon_{cr} E \sqrt{t}} \right) \sqrt{2}. \tag{35}$$

In particular, for a perfect plate all crack parameters may be determined by introducing (28) via Hooke's law from a strain superposition, $\epsilon_{cr} \rightarrow (\epsilon_{cr} - \epsilon_0)$, and the curvature κ by (32). In the case of an imperfection, $u_3^0(x) = ku_3(x)$, affinity will prevail due to the separability in (30) and (31), and by appropriate scaling, $\tilde{\epsilon}_0 = (1+k)\epsilon_0$, the crack parameters may likewise be determined from (34) to be

$$G^* = (\tilde{\epsilon}_0/\epsilon_{cr} - 1)(\tilde{\epsilon}_0/\epsilon_{cr} + 3)/(1+k)^2 \tag{36}$$

and from (35)

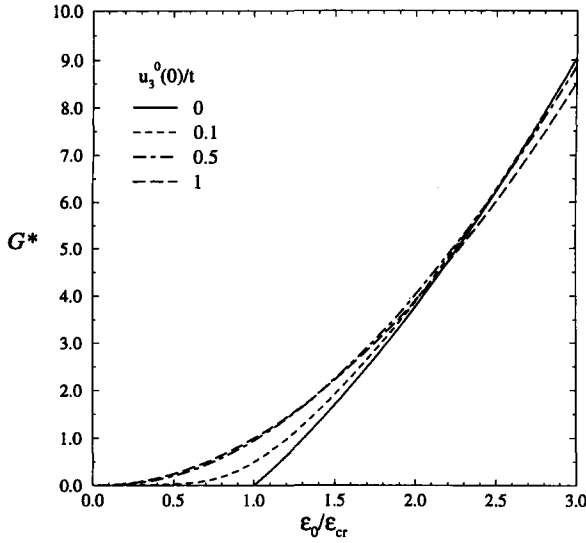


Fig. 6. Energy release rate for a wide plate as a function of load for various imperfections.

$$\begin{pmatrix} K_I^* \\ K_{II}^* \end{pmatrix} = \left[(1 - \tilde{\epsilon}_0/\epsilon_{cr}) \begin{pmatrix} \cos \omega \\ \sin \omega \end{pmatrix} + 2\sqrt{\tilde{\epsilon}_0/\epsilon_{cr} - 1} \begin{pmatrix} \sin \omega \\ -\cos \omega \end{pmatrix} \right] / (1+k). \quad (37)$$

Remembering that the initial imperfection, $\alpha = u_3^0(0)/t$, is related to k by (15), then the crack parameters may be readily determined as a function of ϵ_0 with α as a parameter. Results are given in Figs 6 and 7 for $\alpha = 0, 0.1, 0.5$ and 1.

As may be seen in Fig. 6 the energy release rate may be substantial for loading below the bifurcation load. Thus, at an imperfection size of the plate thickness and crack growth corresponding to the buckling load, a bifurcation analysis would yield a critical postbuckling load in excess of 30%. The same features also prevail for the stress intensity factors as depicted in Fig. 7. It is particularly interesting to notice that mode II becomes more dominant in the postbuckling range, which from a crack growth point of view might be beneficial as ordinarily critical intensities are higher at shearing modes. It is also apparent

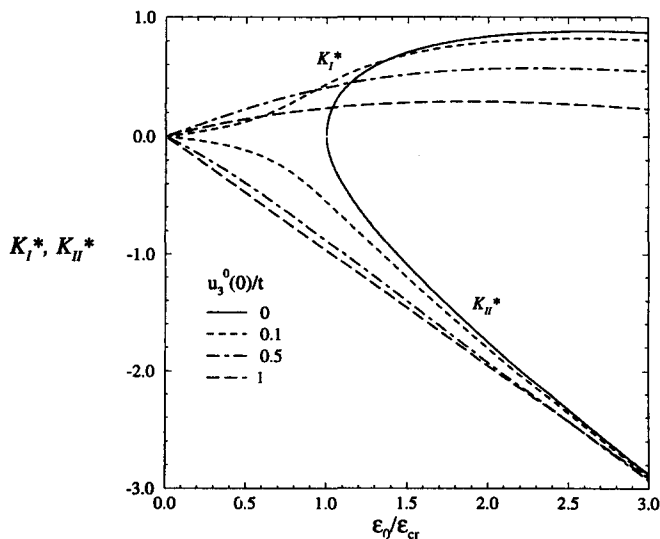


Fig. 7. Stress intensity factors for a wide plate as a function of load for various imperfections.

that at about $\varepsilon_0/\varepsilon_{cr} = 2$, the presence of imperfections is no longer detrimental and no values higher than 3 are displayed. Thus other phenomena might intervene, and it must be remembered that at Euler buckling for instance a potential second bifurcation mode is attainable at $\varepsilon_0/\varepsilon_{cr} = 2.05$. This mode, however, is antisymmetric and will in the present setting be associated with interpenetration of the substrate. Further, at the extreme value of $\varepsilon_0/\varepsilon_{cr} = 7.56$ in the present symmetric case mode K_1 becomes negative which would indicate crack-tip contact. From a physical point of view both issues infer that global and local contact has to be taken into account. Suffice it to say, in this context, that the influence of contact on delamination has recently been subject to a thorough numerical study by Giannakopoulos *et al.* (1991) when contact does not interfere with stability, and by Nilsson and Giannakopoulos (1992) when contact already occurs at initial buckling.

Returning for a moment to Fig. 6 it is evident that for values of the dimensionless energy release rate, G^* , as defined in (34), crack growth will be enhanced by the presence of imperfections when $G^* < 4$, say. It is thus of immediate interest to examine the magnitude of critical values, G_{ξ}^* , in typical situations. To this end, a recent theoretical and experimental investigation of delamination growth in fibre-reinforced carbon/epoxy composites by Nilsson *et al.* (1993) may serve as a basis. Material parameters used were $G_c = 217 \text{ J m}^{-2}$, $E = 146 \text{ GPa}$, $\nu = 0.3$ for unidirectional fibres and delamination thickness $t = 0.381 \text{ mm}$. For a relative thickness $t/L = 0.02$, (29) and (34) then generate $G_{\xi}^* \sim 0.4$. This value is thus definitely in the range when imperfection sensitivity is significant. In the case of other material systems such as ceramic surface layers (Evans *et al.*, 1990) a variety of interface fracture parameters are recorded. In the case of Al_2O_3 -glass the fracture energy was 8 J m^{-2} . Setting $E = 350 \text{ GPa}$, which is a typical value, and using the same geometric parameters as above, the critical value of G_{ξ}^* will be two orders lower than for carbon-fibre epoxy, accentuating the imperfection sensitivity. Although coatings may be as thin as $1 \mu\text{m}$ in some applications, the critical energy release rate will still be in the imperfection sensitivity range.

When an imperfection mode coincides with an eigenmode, as in the present illustration, the results generated are exact within the procedure adopted. This is also the case in other situations of inextensible buckling when amplitudes and modes are separable to first order. This is, however, an exception rather than the rule. In general multidimensional situations, the influence of imperfections will be more intricate.

Retaining for a moment the present one-dimensional situation, at arbitrary imperfection geometries it is expected that the deflection mode will, for sufficiently high loads, converge to the eigenmode. However, at lower loads the imperfection shape might affect the amplitude of the crack parameters. In a recent investigation by Loué (1990), five imperfection shapes were studied. For that purpose two deflection functions were adopted:

$$\begin{aligned} f(x; \xi) &= u_3^0 \left\{ \left(1 + \cos \frac{2\pi x}{L} \right) / 2 + \left[1 - \left(\frac{2x}{L} \right)^\xi \right]^2 \right\} \\ g(x; \xi) &= u_3^0 \left[2 - \left(1 - \frac{2x}{L} \right)^\xi \right] \left[1 - \left(\frac{2x}{L} \right)^\xi \right] \end{aligned} \quad (38)$$

$f(x; \xi)$ representing an imperfection with a high curvature close to the crack front but being flatter elsewhere, whereas $g(x; \xi)$ simulates an imperfection which has a high curvature in the centre but is almost flat elsewhere. These features become more pronounced with increasing ξ . In addition to the buckling mode (20) the shapes of $f(x; 4)$, $f(x; 32)$, $g(x; 4)$ and $g(x; 32)$ were investigated. In particular, for the imperfection level, $u_3^0(0)/t = 0.1$, at the bifurcation load, $\varepsilon_0/\varepsilon_{cr} = 1$, the buckling mode gave an energy release rate 11% and 33% higher than for $f(x; 4)$ and $f(x; 32)$ respectively and energy release rates 13% lower and 10% higher for $g(x; 4)$ and $g(x; 32)$, respectively. Thus, there is no apparent uniform trend in these findings and no reason was found to further elaborate on the matter as regards load and imperfection levels. To obtain a very accurate quantitative result for the energy release rates the true imperfection shape should be used. In practice, however, exact shapes are seldom known.

5.2. A circular thin plate on a substrate under axisymmetric compression

As a prelude it was shown in the analysis of a one-dimensional case that exact determination of relevant parameters may be pursued by the adopted imperfection analysis. In two-dimensional situations this is not generally so and it seems appropriate next to analyse specifically the influence of imperfections of a circular delamination under axisymmetric compressive loading. In particular, the accuracy involved in adopting the proposed scaling procedure is at issue.

On assuming axisymmetry at postbuckling the problem essentially reduces analytically to a one-dimensional case. The geometry and loading is therefore depicted as in Fig. 5 by symmetry analogy and only an obvious change of notation. Proceeding, then, determination of energy release rates at postbuckling has been carried out earlier by, for example, Evans and Hutchinson (1984) using an asymptotic method and by Yin (1985) using a Rayleigh-Ritz method in conjunction with a shooting technique. Then, in order to determine imperfection sensitivity the results of Yin (1985) may be drawn upon directly by scaling. Presently, however, in order to cover a sufficiently large loading range at scaling, a p -version of a finite element method proposed by Storåkers and Andersson (1988) was applied.

The approach proceeds much in parallel with the truly one-dimensional situation. A thin plate is clamped to a thick substrate, the latter being under uniform compression:

$$\varepsilon_{rr} = \varepsilon_{\phi\phi} = -\varepsilon_0, \quad (39)$$

where ε_0 is prescribed.

Buckling of a perfect Hookean plate will initiate at

$$\varepsilon_{cr} = \frac{1.22}{1+\nu} \left(\frac{t}{a} \right)^2, \quad (40)$$

[cf. e.g. Thompson and Hunt (1973)]. The associated transverse deflection mode is

$$u_3(r) = \frac{J_0(\gamma a) - J_0(\gamma r)}{J_0(\gamma a) - 1}, \quad (41)$$

where J_0 is the first Bessel function of zero order and $\gamma = 3.83/a$, as for a clamped plate.

Now, given the presence of an affine imperfection and in analogy with the wide plate problem dealt with above, the relevant fracture parameters are, by (26) and (27) using (34) and (35),

$$G^* = \left(\frac{(\tilde{\varepsilon}_{rr} + \tilde{\varepsilon}_0)^2}{(1+k)^2} + \frac{(\tilde{\kappa}_{rr}t)^2}{(1+k)(1+2k)} \right) / \varepsilon_{cr}^2, \quad (42)$$

and

$$\begin{pmatrix} K_I^* \\ K_{II}^* \end{pmatrix} = \left[-\frac{(\tilde{\varepsilon}_{rr} + \tilde{\varepsilon}_0)}{(1+k)} \begin{pmatrix} \cos \omega \\ \sin \omega \end{pmatrix} + \frac{\tilde{\kappa}_{rr}t}{\sqrt{(1+k)(1+2k)}} \begin{pmatrix} \sin \omega \\ -\cos \omega \end{pmatrix} \right] / \varepsilon_{cr}, \quad (43)$$

where $\tilde{\varepsilon}_{rr}$ and $\tilde{\kappa}_{rr}$ denote the membrane strain and curvature respectively in the postbuckling solution for a perfect plate.

As has already been predicted the deflected shape of the plate will vary as a function of the load at postbuckling. Thus, deflection affinity will not prevail in general and when drawing on the scaling procedure, exact results will only be expected when deflected shapes happen to coincide with initially imperfect ones. At approximate estimates then it is natural to scale imperfections with the aid of the central deflection, $u_3(0)$. Accepting this as a basis, relevant crack-tip parameters are then readily determined from the FEM-analysis of the perfect plate.

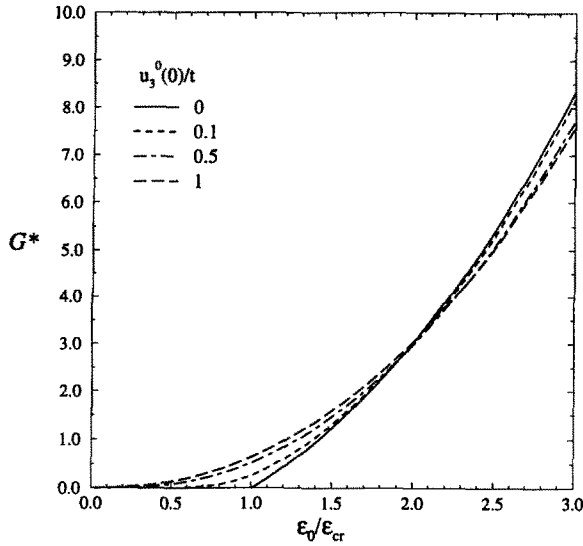


Fig. 8. Energy release rate for a circular plate under axisymmetric compression as a function of load for various imperfections.

In analogy with the wide-plate case above, energy release rates and crack intensity factors are given in Figs 8 and 9 respectively as functions of the loading for different imperfection magnitudes. As may be seen, very similar conclusions may be drawn as shown above for the wide-plate case in Figs 6 and 7. Although not explicitly exhibited in Fig. 9, at higher loading the mode I stress intensity factor, K_I^* , will reach a maximum and then level off slowly. It will, however, not change sign and hence no crack-tip contact is to be expected within the von Karman kinematics adopted.

Of more interest then is the approximate character of the imperfection approach. In order to assess the accuracy, a comparison was made between stress intensity factors based on the direct scaling procedure and on a nonlinear FEM-analysis with the initial buckling mode as an imperfection. The results are depicted in Fig. 10 for an initially perfect plate

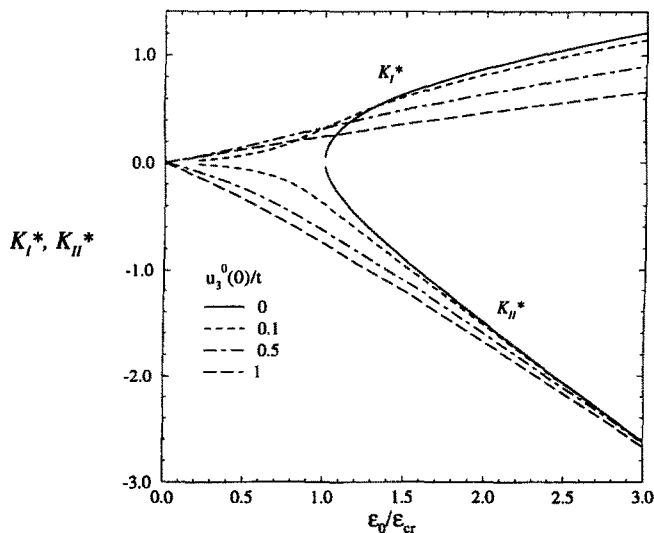


Fig. 9. Stress intensity factors for a circular plate under axisymmetric compression as a function of load for various imperfections.

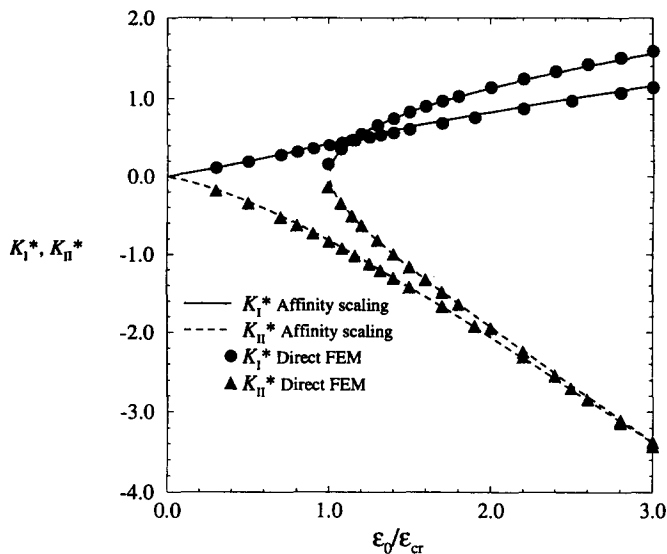


Fig. 10. Comparison of stress intensity factors at bifurcation and by direct scaling from an infinite element analysis for an imperfection, $u_3^0(t)/t = 0.5$.

and a chosen imperfection $u_3(0)/t = 0.5$. For the load range considered the results virtually coincide.

5.3. A circular thin plate on a substrate under uniaxial compression

A more intricate problem is to determine stress intensity factors at buckling with a circular crack contour while the compressive load is nominally uniaxial. Full symmetry is then lost and in particular self-similarity of crack growth is not to be expected.

In this case a commercial FEM-code, SOLVIA, was used for the scaling procedure at postbuckling. The mesh adopted is shown in Fig. 11 where one quarter of the circular plate

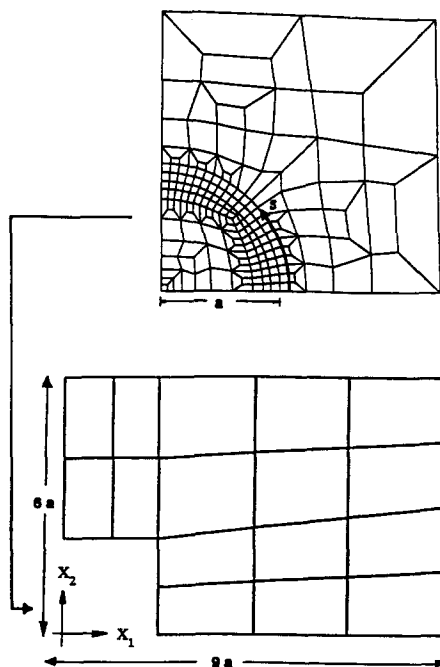


Fig. 11. FE-mesh used for a circular delamination.

is modelled. At the crack contour the plate is clamped while remotely in the substrate the loading is imposed by

$$\begin{aligned} u_3 = -9a\epsilon_0, \quad N_{12} = 0 \quad \text{at} \quad x_1 = 9a, \\ N_{2x} = 0 \quad \text{at} \quad x_2 = 6a, \end{aligned} \quad (44)$$

together with the appropriate symmetry conditions along $x_1, x_2 = 0$.

In the present setting the problem has been analysed earlier for perfect plates by Nilsson and Giannakopoulos (1990) where the distribution of energy release rates was derived and subsequent nontrivial growth was simulated and by Nilsson and Storåkers (1991) where also the distribution of stress intensity factors were calculated. Some pertinent results are first reproduced for the case of a perfect plate.

The stress intensity factor K_{III} was found to vanish almost completely. In Fig. 12 the remaining stress intensity factors are shown along the crack contour for two loading values, $\epsilon_0/\epsilon_{cr} = 1.03$ and 1.28, where the bifurcation buckling load was found to be $\epsilon_{cr} = 2.52 (t/a)^2$ for Poisson's ratio $\nu = 0.3$. A curve parameter, s , is introduced along the crack front where s varies from 0 to 1 as also indicated in Fig. 11 above. It is evident that stress intensity factors vary in a nontrivial manner attaining the largest values at $s = 1$, i.e. transverse to the imposed loading. In Fig. 13 stress intensities are shown at $s = 0, 1$ as a function of the loading and it may be seen that at $s = 0$, K_I^* vanishes for $\epsilon_0 = 1.28\epsilon_{cr}$. Accordingly crack-tip contact is to be expected at higher loading. In the present context in particular deflected shapes at postbuckling will then be locally affected. It is clear, however, from Figs 12 and 13 that high values of stress intensity factors originate in regions remote from the predicted contact.

As a representative case, in Fig. 14 stress intensity factors along the delamination front are shown for an imperfection of $u_3^0(0)/t = 0.5$ and at an applied loading $\epsilon_0/\epsilon_{cr} = 0.36$, i.e. below the buckling load. Results have been determined both by the scaling method and by a full nonlinear FEM-analysis with the bifurcation buckling mode used as an initial imperfection. On the whole the two imperfection approaches give results that are very similar. It may be observed, however, that already at this pre-bifurcation load, K_I^* is negative although only in the vicinity where stress intensity factors are small. In a strict sense these results are physically unacceptable due to predicted interpenetration. In the recent combined theoretical and experimental study of delamination growth by Nilsson *et*

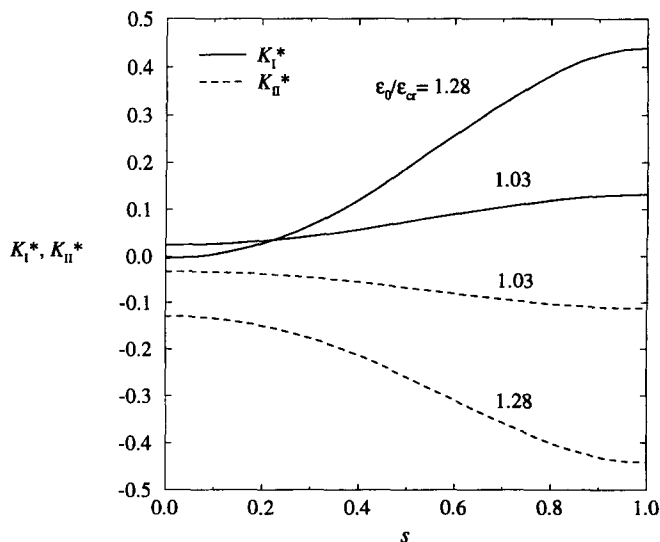


Fig. 12. Stress intensity factors along a circular delamination front for a perfect plate under uniaxial compression at two load levels.

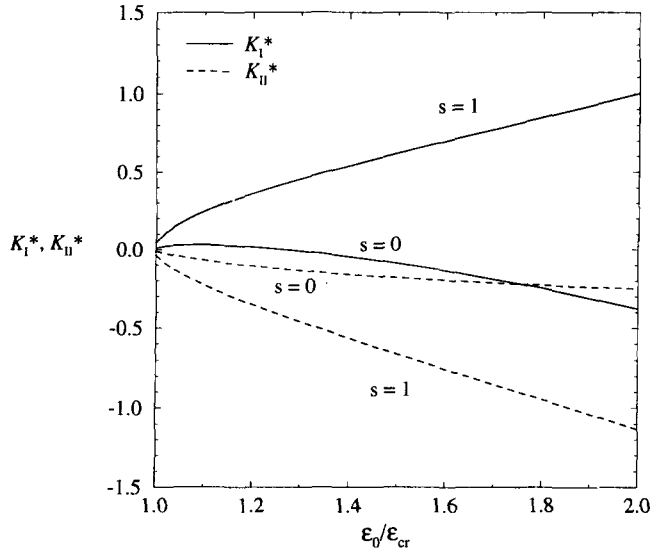


Fig. 13. Stress intensity factors normal, $s = 0$, and transverse, $s = 1$, to the loading direction as a function of uniaxial compressive loading.

al. (1993) it was found, however, that the shape of the delamination was not much affected by the contact provided that crack growth is expected remote from a contact region. The magnitude of crack parameters was affected, although only slightly.

Thus, suppressing this anomaly, as in the two systems analysed above, crack parameters are given as functions of the loading for different imperfection magnitudes. In Fig. 15 the energy release rates are given at $s = 0, 1$, as functions of the imposed loading and in Fig. 16 the associated stress intensity factors. The initially perfect plate was only loaded up to $4\epsilon_{cr}$. Again the influence of an initial imperfection shows the same features as above for wide-plate buckling and axisymmetric buckling. Further, in Fig. 17, it is demonstrated that the simple scaling method also, in this case, is quite sufficient to achieve accuracy as compared to a full FEM-analysis.

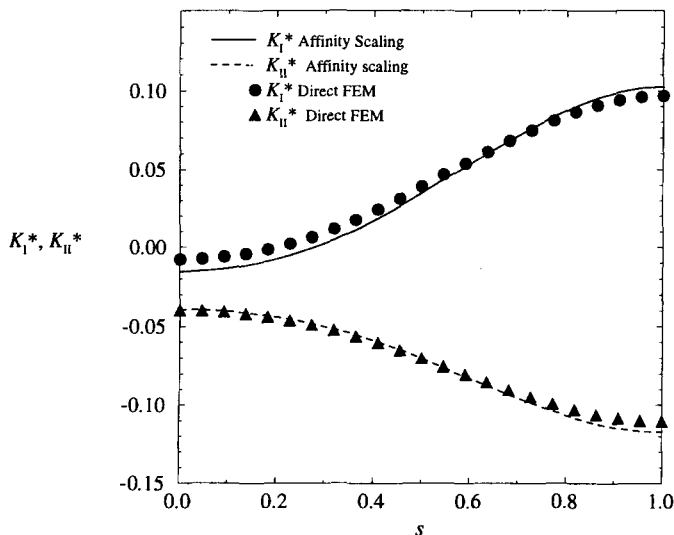


Fig. 14. Comparison of distribution of stress intensity factors by direct scaling and by finite element analysis for a circular plate under nominal uniaxial compression for an imperfection, $u_3^0(t)/t = 0.5$.

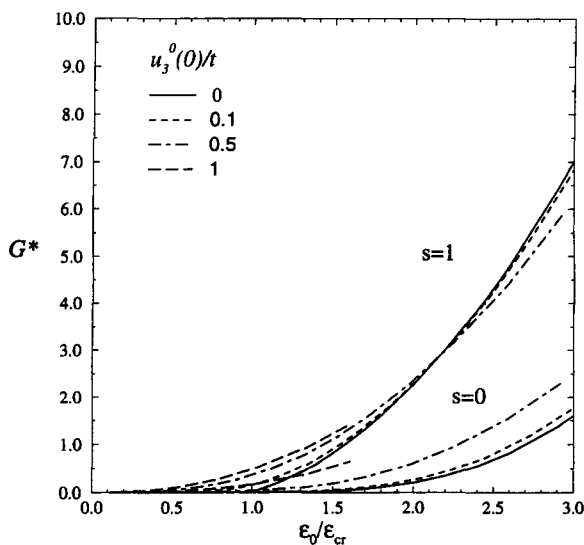


Fig. 15. Energy release rate for a circular plate under nominal uniaxial compression as a function of load for various imperfections.

Finally, for the two cases of a circular delamination it may be concluded from Figs 8 and 15 respectively that the presence of imperfections will enhance crack growth when $G^* < 3$ say. With eqn (34) and the just determined values of ϵ_{cr} it is evident that the role of imperfections for circular contours will be of similar significance for laminates of specific materials as illustrated for the wide-plate previously.

6. CONCLUDING REMARKS

A useful analytical scaling procedure was proposed to generate crack parameters at buckling for imperfect plates from perfect ones. The method assumes transverse deflections and initial imperfections to be affine and in such a case exact results may be directly read

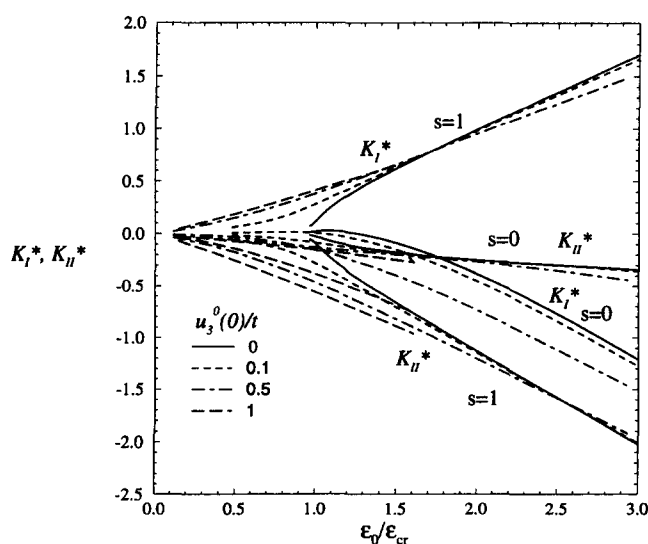


Fig. 16. Stress intensity factors for a circular plate under nominal uniaxial compression as a function of load for various imperfections.

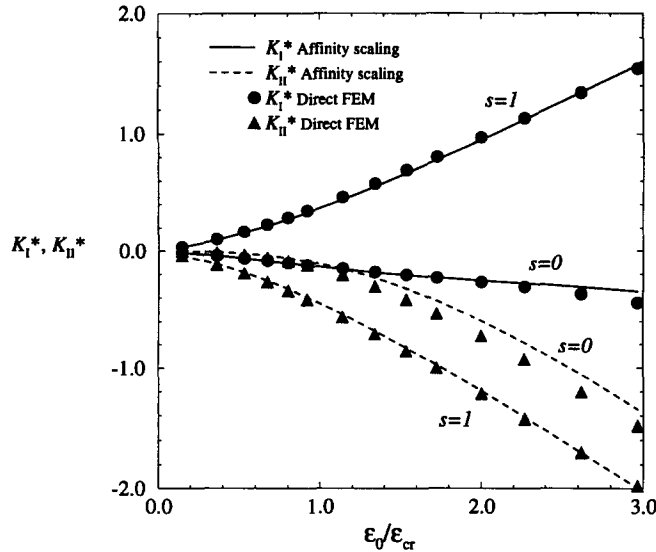


Fig. 17. Comparison of stress intensity factors normal, $s = 0$, and transverse, $s = 1$, to the loading by direct scaling and by finite element analysis for an imperfection, $u_3(0)/t = 0.5$.

off from existing ones for a perfect plate. In other situations approximate results were found to be within very good accuracy for representative cracks.

The presence of initial imperfections is believed to be of notable importance at delamination buckling and growth as it was found that predicted crack growth may very well precede the event of bifurcation buckling. For the cases analysed, with imperfection amplitudes ascending to the plate thickness, it was concluded that only at load levels higher than around twice the bifurcation load did the consequences become insignificant and in fact turn favourable.

REFERENCES

- Abrate, S. (1991). Impact on laminated composite materials. *Appl. Mech. Rev.* **44**, 155–190.
- Chai, H., Babcock, C. D. and Knauss, W. G. (1981). One-dimensional modeling of failure in laminated plates by delamination buckling. *Int. J. Solids Structures* **17**, 1069–1083.
- Chai, H., Knauss, W. G. and Babcock, C. D. (1983). Observation of damage growth in compressively loaded laminates. *Exp. Mech.* **30**, 329–337.
- Chia, C.-Y. (1980). *Nonlinear Analysis of Plates*. McGraw-Hill, New York.
- Cotterell, B., Kamminga, J. and Dickson, F. P. (1985). The essential mechanics of conchoidal flaking. *Int. J. Fract.* **29**, 101–119.
- Evans, A. G. and Hutchinson, J. W. (1984). On the mechanics of delamination and spalling in compressed films. *Int. J. Solids Structures* **20**, 455–466.
- Evans, A. G., Rühle, M., Dahlgleich, B. J. and Charalambides, P. G. (1990). The fracture energy of bimaterial interfaces. *Mater. Sci. Engng A* **126**, 53–64.
- Garg, A. C. (1988). Delamination—A damage mode in composite structures. *Engng Fract. Mech.* **29**, 557–584.
- Giannakopoulos, A. E., Tsamasphyros, G. and Nilsson, K.-F. (1991). The contact problem at delamination, part 1. Report -137, Department of Solid Mechanics, Royal Institute of Technology, S-100 44 Stockholm, Sweden.
- Gillespie, J. W. Jr and Carlsson, L. A. (1991). Buckling and growth of delamination in thermoset and thermoplastic composites. *J. Engng Mater. Technol.* **113**, 93–98.
- Hutchinson, J. W. and Suo, Z. (1992). Mixed mode cracking in layered materials. *Adv. Appl. Mech.* **28**, 63–191.
- Koiter, W. T. (1945). Over de stabiliteit van het elastisch evenwicht. Ph.D-Thesis, Delft, H.J. Paris, Amsterdam. (On the stability of elastic equilibrium, English translation issued by NASA, TT F-10, 833, 1967.)
- Larsson, P. L. (1991). On multiple delamination buckling and growth in composite plates. *Int. J. Solids Structures* **27**, 1623–1637.
- Lekhnitskii, S. G. (1981). *Theory of Elasticity of an Anisotropic Body* (English translation). Mir Publishers, Moscow.
- Librescu, L. and Chang, M.-Y. (1992). Imperfection sensitivity and postbuckling behavior of shear-deformable composite doubly-curved shallow panels. *Int. J. Solids Structures* **29**, 1065–1083.
- Loué, P. (1990). Sensitivity of delaminations to initial imperfections in one-dimensional laminated plates. M.Sc.Thesis, Ecole Polytechnique, Palaiseau, France.
- Marguerre, K. (1938). Zur Theorie der gekrümmten Platte grosser Formänderungen. *Proc. 5th Int. Congr. Appl. Mech.*, pp. 93–101. Wiley, New York.

- Nilsson, K.-F. and Giannakopoulos, A. E. (1990). Finite element simulation of delamination growth. In *Proceedings of the First International Conference on Computer-Aided Assessment and Control of Localized Damage* (Edited by M. H. Aliabadi, C. A. Brebbia and D. J. Cartwright), pp. 299–313. Springer, Berlin.
- Nilsson, K.-F. and Giannakopoulos, A. E. (1992). The contact problem in delamination, part 2. Report-141, Department of Solid Mechanics, Royal Institute of Technology, S-100 44, Stockholm, Sweden.
- Nilsson, K.-F. and Storåkers, B. (1992). On interface crack growth in composite plates. *J. Appl. Mech.* **59**, 530–538.
- Nilsson, K.-F., Thesken, J.-C., Sindelar, P., Giannakopoulos, A. E. and Storåkers, B. (1993). A theoretical and experimental investigation of buckling induced delamination growth. *J. Mech. Phys. Solids* (in press).
- Nyländer, H. (1951). Initially deflected thin plate with initial deflection affine to additional deflection. *Int. Assoc. Bridge Struct. Engng* **11**, 347–374.
- Rice, J. R. (1988). Elastic fracture mechanics concepts for interfacial cracks. *J. Appl. Mech.* **55**, 98–103.
- Schapery, R. A. and Davidson, B. D. (1990). Prediction of energy release rates for mixed mode delamination using classical plate theory. Report no MM. 9045-90-3, Texas A&M University, College Station, Texas, U.S.A.
- Storåkers, B. (1989). Nonlinear aspects of delamination in structural members. In *Proceedings of the 17th International Congress of Theoretical and Applied Mechanics* (Edited by P. Germain, M. Piau and D. Caillerie), pp. 315–336. Elsevier, Amsterdam.
- Storåkers, B. and Andersson, B. (1988). Nonlinear plate theory applied to delamination in composites. *J. Mech. Phys. Solids* **36**, 689–718.
- Suo, Z. (1990a). Singularities, interfaces, and cracks in dissimilar anisotropic media. *Proc. Roy. Soc. Lond.* **A427**, 331–358.
- Suo, Z. (1990b). Delamination specimens for orthotropic materials. *J. Appl. Mech.* **57**, 627–634.
- Suo, Z. and Hutchinson, J. W. (1990). Interface crack between two elastic layers. *Int. J. Fract.* **43**, 1–18.
- Thompson, J. M. T. and Hunt, G. W. (1973). *A General Theory of Elastic Stability*. Wiley, New York.
- Thouless, M. D., Evans, A. G., Ashby, M. F. and Hutchinson, J. W. (1987). The edge cracking and spalling of brittle plates. *Acta Metall.* **35**, 1333–1341.
- Whitcomb, J. D. (1986). Parametric analytical study of instability related delamination growth. *Compos. Sci. Technol.* **20**, 19–48.
- Yin, W. L. (1985). Axisymmetric buckling and growth of a circular delamination in a compressed laminate. *Int. J. Solids Structures* **21**, 503–514.